Search for η-mesic ^{4}He with the WASA-at-COSY detector

P. Adlarson,[1] W. Augustyniak,[2] W. Bardan,[3] M. Bashkanov,[4] T. Bednarski,[3] F. S. Bergmann,[5] M. Berłowski,[6] H. Bhatt,[7] M. Büscher,[8,9] H. Calén,[1] H. Clement,[4] D. Coderre,[8,9,10] E. Czerwiński,[3] K. Demmich,[5] E. Doroshkevich,[4] R. Engels,[8,9] W. Erven,[9,11] W. Eyrich,[12] P. Fedorets,[8,9,13] K. Föhl,[14] K. Fransson,[1] F. Goldenbaum,[8,9] P. Goslawski,[5] A. Goswami,[15] K. Grigoryev,[8,9,16] C.–O. Gullström,[1] F. Hauenstein,[12] L. Heijkenskjöld,[1] V. Hejny,[8,9] F. Hinterberger,[17] M. Hodana,[3,8,9] B. Höistad,[1] A. Jany,[3] B. R. Jany,[3] L. Jarczyk,[3] T. Johansson,[1] B. Kamys,[3] G. Kemmerling,[9,11] F. A. Khan,[8,9] A. Khoukaz,[5] S. Kistryn,[3] J. Klaja,[3] H. Kleines,[9,11] B. Kłos,[18] M. Krapp,[12] W. Krzemień,[3] P. Kulessa,[19] A. Kupść,[1,6] K. Lalwani,[7] D. Lersch,[8,9] L. Li,[12] B. Lorentz,[8,9] A. Magiera,[3] R. Maier,[8,9] P. Marciniewski,[1] B. Mariański,[2] M. Mikirtychiants,[8,9,10,16] H.–P. Morsch,[2] P. Moskal,[3] B. K. Nandi,[7] S. Niedźwiecki,[3] H. Ohm,[8,9] I. Ozerianska,[3] E. Perez del Rio,[4] P. Pluciński,[1,*] P. Podkopał,[3,8,9] D. Prasuhn,[8,9] A. Pricking,[4] D. Pszczel,[1,6] K. Pysz,[19] A. Pyszniak,[1,3] C. F. Redmer,[1,†] J. Ritman,[8,9,10] A. Roy,[15] Z. Rudy,[3] S. Sawant,[7] S. Schadmand,[8,9] A. Schmidt,[12] T. Sefzick,[8,9] V. Serdyuk,[8,9,20] N. Shah,[7,‡] M. Siemaszko,[18] R. Siudak,[19] T. Skorodko,[4] M. Skurzok,[3] J. Smyrski,[3] V. Sopov,[13] R. Stassen,[8,9] J. Stepaniak,[6] E. Stephan,[18] G. Sterzenbach,[8,9] H. Stockhorst,[8,9] H. Ströher,[8,9] A. Szczurek,[19] T. Tolba,[8,9,§] A. Trzciński,[2] R. Varma,[7] P. Vlasov,[17] G. J. Wagner,[4] W. Węglorz,[18] M. Wolke,[1] A. Wrońska,[3] P. Wüstner,[9,11] P. Wurm,[8,9] A. Yamamoto,[21] X. Yuan,[22] L. Yurev,[20,‖] J. Zabierowski,[23] C. Zheng,[22] M. J. Zieliński,[3] W. Zipper,[18] J. Złomańczuk,[1] P. Żuprański,[2] and M. Żurek[3]

(WASA-at-COSY Collaboration)

[1]*Division of Nuclear Physics, Department of Physics and Astronomy, Uppsala University, Box 516, 75120 Uppsala, Sweden*
[2]*Department of Nuclear Physics, National Centre for Nuclear Research, ulica Hoza 69, 00-681, Warsaw, Poland*
[3]*Institute of Physics, Jagiellonian University, ulica Reymonta 4, 30-059 Kraków, Poland*
[4]*Physikalisches Institut, Eberhard-Karls-Universität Tübingen, Auf der Morgenstelle 14, 72076 Tübingen, Germany*
[5]*Institut für Kernphysik, Westfälische Wilhelms-Universität Münster, Wilhelm-Klemm-Strasse 9, 48149 Münster, Germany*
[6]*High Energy Physics Department, National Centre for Nuclear Research, ulica Hoza 69, 00-681, Warsaw, Poland*
[7]*Department of Physics, Indian Institute of Technology Bombay, Powai, Mumbai 400076, Maharashtra, India*
[8]*Institut für Kernphysik, Forschungszentrum Jülich, 52425 Jülich, Germany*
[9]*Jülich Center for Hadron Physics, Forschungszentrum Jülich, 52425 Jülich, Germany*
[10]*Institut für Experimentalphysik I, Ruhr-Universität Bochum, Universitätsstrasse 150, 44780 Bochum, Germany*
[11]*Zentralinstitut für Elektronik, Forschungszentrum Jülich, 52425 Jülich, Germany*
[12]*Physikalisches Institut, Friedrich-Alexander-Universität, Erlangen-Nürnberg, Erwin-Rommel-Strasse 1, 91058 Erlangen, Germany*
[13]*Institute for Theoretical and Experimental Physics, State Scientific Center of the Russian Federation, Bolshaya Cheremushkinskaya 25, 117218 Moscow, Russia*
[14]*II. Physikalisches Institut, Justus-Liebig-Universität Giessen, Heinrich-Buff-Ring 16, 35392 Giessen, Germany*
[15]*Department of Physics, Indian Institute of Technology Indore, Khandwa Road, Indore 452017, Madhya Pradesh, India*
[16]*High Energy Physics Division, Petersburg Nuclear Physics Institute, Orlova Rosha 2, 188300 Gatchina, Russia*
[17]*Helmholtz-Institut für Strahlen- und Kernphysik, Rheinische Friedrich-Wilhelms-Universität Bonn, Nussallee 14-16, 53115 Bonn, Germany*
[18]*August Chełkowski Institute of Physics, University of Silesia, Uniwersytecka 4, 40-007, Katowice, Poland*
[19]*The Henryk Niewodniczański Institute of Nuclear Physics, Polish Academy of Sciences, 152 Radzikowskiego Street, 31-342 Kraków, Poland*
[20]*Dzhelepov Laboratory of Nuclear Problems, Joint Institute for Nuclear Physics, Joliot-Curie 6, 141980 Dubna, Russia*
[21]*High Energy Accelerator Research Organisation KEK, Tsukuba, Ibaraki 305-0801, Japan*
[22]*Institute of Modern Physics, Chinese Academy of Sciences, 509 Nanchang Road, 730000 Lanzhou, China*
[23]*Department of Cosmic Ray Physics, National Centre for Nuclear Research, ulica Uniwersytecka 5, 90-950 Łódź, Poland*

An exclusive measurement of the excitation function for the $dd \to {}^3\mathrm{He}\, p\pi^-$ reaction was performed at the Cooler Synchrotron COSY-Jülich with the WASA-at-COSY detection system. The data were taken during a slow acceleration of the beam from 2.185 to 2.400 GeV/c crossing the kinematic threshold for the η-meson production in the $dd \to {}^4\mathrm{He}\,\eta$ reaction at 2.336 GeV/c. The corresponding excess energy with respect to the ^{4}He-η system varied from -51.4 to 22 MeV. The integrated luminosity in the experiment was determined using the $dd \to {}^3\mathrm{He}\,n$ reaction. The shape of the excitation function for the $dd \to {}^3\mathrm{He}\,p\pi^-$ reaction was examined. No signal of the ^{4}He-η bound state was observed. An upper limit for the cross section for the bound state formation and decay in the process $dd \to ({}^4\mathrm{He}\text{-}\eta)_{\mathrm{bound}} \to {}^3\mathrm{He}\,p\pi^-$ was determined on the 90% confidence level and it varies from 20 to 27 nb for the bound state width ranging from 5 to 35 MeV, respectively.

*Present address: Department of Physics, Stockholm University, Roslagstullsbacken 21, AlbaNova, 10691 Stockholm, Sweden.

†Present address: Institut für Kernphysik, Johannes Gutenberg-Universität Mainz, Johann-Joachim-Becher Weg 45, 55128 Mainz, Germany.

I. INTRODUCTION

Neutral mesons, such as η, K, ω, and η', can potentially form bound states with atomic nuclei. In this case the binding is exclusively due to the strong interaction and the bound state or *mesic nucleus* can be considered as a meson captured in the mean field of the nucleons. Due to the strong attractive η-nucleon interaction [1,2], the η-mesic nuclei are some of the most promising candidates for such states.

Experimental confirmation of the existence of η-mesic nuclei would be interesting on its own but it would be also valuable for investigations of the η-N interaction and for the study of in-medium properties of the N^* resonance [3] and of the η meson [4]. It could also help to determine the flavor singlet component of the η wave function [5].

The existence of η-mesic nuclei was postulated in 1986 by Haider and Liu [6]. Experimental searches have been performed by several past experiments [7–11] while ongoing investigations continue at COSY [12–17], JINR [18], J-PARC [19], and MAMI [20] and are planned at GSI [21]. Many promising indications have been reported; however, so far there is no direct experimental confirmation of the existence of mesic nuclei.

In the region of light nuclei systems such as η-He the observation of a strong enhancement in the total production cross section and the phase variation of the scattering amplitude in the close-to-threshold region has provided strong evidence for the existence of a pole in the scattering matrix which can correspond to a bound state [22]. In particular, a very strong final state interaction (FSI) is observed in the $dd \rightarrow {}^4$Heη reaction close to kinematic threshold and is interpreted as a possible indication of the ^{4}He-η bound state [23]. This suggests that the ^{4}He-η system is a good candidate for the experimental study of a possible binding. This conclusion is strengthened by the predictions in Ref. [1].

However, as stated in Refs. [24,25], the theoretical predictions for the width and binding energy of the η-mesic nuclei are strongly dependent on the subthreshold η-nucleon interaction, which is not well understood. Therefore, direct measurements that could confirm the existence of the bound state are mandatory.

Taking into account the above arguments and the fact that in light nuclei systems the bound states are expected to be much narrower compared to the case of heavy nuclei [26], we performed a search for η-mesic ^{4}He at the Cooler Synchrotron COSY-Jülich with the WASA-at-COSY detector [27].

II. EXPERIMENT

The experiment was based on the measurement of the excitation function of the $dd \rightarrow {}^3$He$p\pi^-$ reaction for energies in the vicinity of the η production threshold and on the selection of events with low ^{3}He center-of-mass (c.m.) momenta. In the case of existence of the ^{4}He-η bound state we expected to observe a resonance-like structure in the excitation function below the threshold for the production of the ^{4}He-η system. The structure would indicate a $dd \rightarrow ({}^4$He-$\eta)_{\text{bound}} \rightarrow {}^3Hep\pi^-$ reaction appearing on the continuous background originating from the direct $dd \rightarrow {}^3$He$p\pi^-$ process.

We expect that the decay of such a state proceeds via the absorption of the η meson on one of the nucleons in the ^{4}He nucleus leading to the excitation of the N^* (1535) resonance which subsequently decays in the pion-nucleon pair. The remaining three nucleons play the role of spectators and they are likely to bind forming a ^{3}He or a ^{3}H nucleus. In the case of a similar system, the ${}^4_\Lambda$He hypernucleus, it was observed that in the π^--decay channel the decay mode ${}^4_\Lambda$He $\rightarrow {}^3$He$p\pi^-$ is dominant [28].

According to the discussed model, there exist four equivalent decay channels of the $({}^4$He-$\eta)_{\text{bound}}$ state:

(1) $({}^4$He-$\eta)_{\text{bound}} \rightarrow {}^3Hep\pi^-$,
(2) $({}^4$He-$\eta)_{\text{bound}} \rightarrow {}^3Hen\pi^0$,
(3) $({}^4$He-$\eta)_{\text{bound}} \rightarrow {}^3Hp\pi^0$,
(4) $({}^4$He-$\eta)_{\text{bound}} \rightarrow {}^3Hn\pi^+$.

In the reported experiment we concentrated on the ^{3}He$p\pi^-$ decay mode.

The WASA-at-COSY detector is described in detail in Refs. [29,30]. It consists of two main parts: the forward detector, dedicated to the measurement of forward-scattered projectiles and target-recoils, and the central detector, optimized for measuring of photons, electrons, and pions originating from decays of mesons and excited baryonic states. The forward part consists of several layers of plastic scintillators
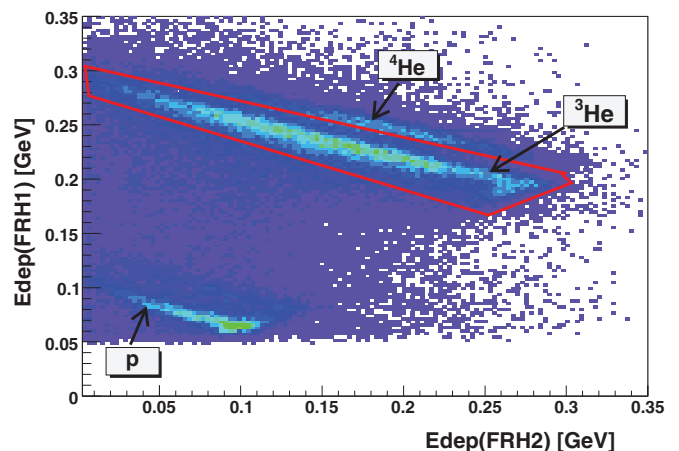

FIG. 1. (Color online) Experimental spectrum of the energy losses in the first two layers of the forward range hodoscope (FRH). The area used for ^{3}He identification is indicated by the red (solid) line. The empty area below 0.05 GeV in the Edep(FRH1) distribution is due to the preselection condition. The regions corresponding to protons, ^{3}He, and ^{4}He are clearly visible.

‡Present address: Department of Physics and Astronomy, University of California, Los Angeles, California 90045, USA.

§Present address: Albert Einstein Center for Fundamental Physics, Fachbereich Physik und Astronomie, Universität Bern, Sidlerstrasse 5, 3012 Bern, Switzerland.

$^\parallel$Present address: Department of Physics and Astronomy, University of Sheffield, Hounsfield Road, Sheffield, S3 7RH, United Kingdom.

allowing for particle identification on the basis of the ΔE-E and ΔE-ΔE information and a proportional drift chamber providing track coordinates. The central detector is composed of an electromagnetic calorimeter, a cylindrical drift chamber, and a barrel of plastic scintillators. A superconducting solenoid provides a magnetic field for momentum determination of the tracks of charged particles measured in the drift chamber. The scintillators provide fast signals for the first level trigger and, together with the drift chamber and the calorimeter, are used for charged particle identification via ΔE-p and ΔE-E methods. WASA-at-COSY uses an internal target system which provides pellets of frozen hydrogen or deuterium. During the present experiment the cooling system of the superconducting solenoid was broken and, therefore, no magnetic field was provided.

During the experimental run the momentum of the deuteron beam was varied continuously within each acceleration cycle from 2.185 GeV/c to 2.400 GeV/c, crossing the kinematic threshold for η production in the $dd \rightarrow {}^4$Heη reaction at 2.336 GeV/c. This range of beam momenta corresponds to a variation of ^{4}He-η excess energy from -51.4 to 22 MeV.
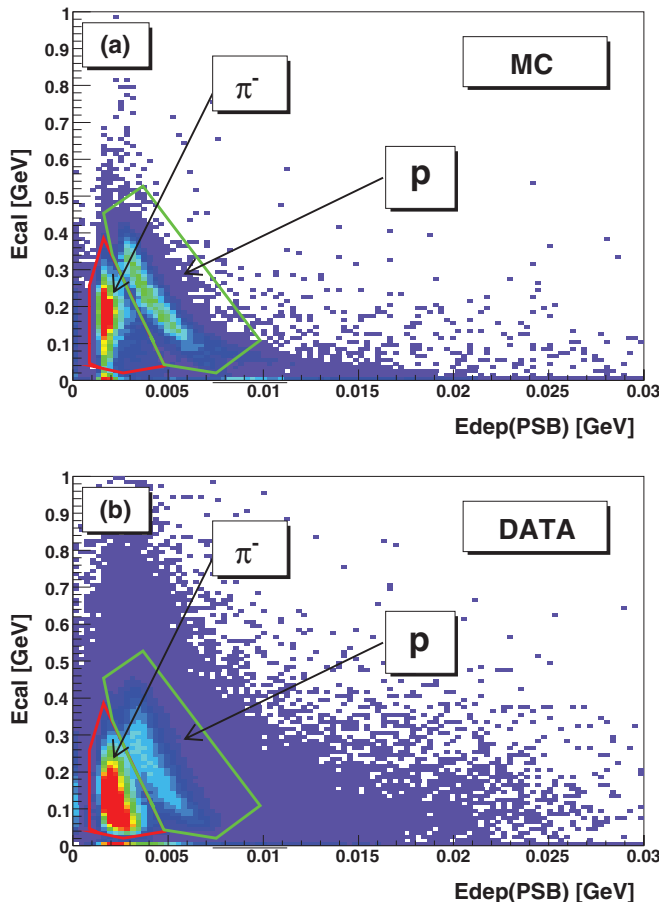

FIG. 2. (Color online) Comparison of the Monte Carlo simulation (a) and the experimental spectrum (b) of the energy loss in the plastic scintillator barrel (x axis) combined with the energy deposited in the electromagnetic calorimeter (y axis). The green (light gray) and red (dark gray) curves represent the applied graphical condition to separate protons and pions.

The identification of the ^{3}He was conducted using the ΔE-ΔE technique, comparing the energy losses in two layers of the forward range hodoscope(FRH) (Fig. 1).

The energy loss in the plastic scintillator barrel was combined with the energy deposited in the electromagnetic calorimeter to identify protons and pions (Fig. 2).

The outgoing ^{3}He nucleus plays the role of a spectator and, therefore, we expect that its momentum in the c.m. frame is relatively low and can be approximated by the Fermi momentum distribution of nucleons inside the ^{4}He nucleus. This signature allows us to suppress background from reactions leading to the ^{3}He$p\pi^-$ final state but proceeding without formation of the intermediate $(^4$He-$\eta)_{\text{bound}}$ state and, therefore, resulting on the average in much higher c.m. momenta of ^{3}He (see Fig. 3).

Therefore, we compare the excitation functions for the $dd \rightarrow {}^3$He$p\pi^-$ reaction from the "signal-rich" region corresponding to the ^{3}He c.m. momenta below 0.3 GeV/c and the "signal-poor" region for the ^{3}He c.m. momenta above 0.3 GeV/c. The number of events as a function of the beam momentum is shown in Fig. 4. At this stage of the analysis the excitation function is not normalized to the luminosity and it is not corrected for reconstruction efficiency. The obtained functions for both regions are smooth and no clear signal, which could be interpreted as a resonance-like structure, is visible. We checked also for possible structures in the difference between the excitation functions for the signal-rich and signal-poor region. We multiplied the function for the signal-poor region by a factor chosen in such a way, that the difference of the two functions for the second bin of Q is equal to zero. This difference is presented in Fig. 4(c) to examine the shape of the excitation function before any further selection criteria are applied. The obtained dependence is flat and is consistent with zero. No resonance structure is visible.

In addition, further observables were taken into account to reduce the background. Additional selection criteria on the p and π^- kinetic energy distributions and the p-π^- opening angle in the c.m. system were applied. In the N^* rest frame this angle is exactly equal to 180° but due to the Fermi motion it is smeared by about 30° in the reaction c.m. system (see Fig. 5). We also applied a condition to the relative p-π^- angle in the c.m. system in the range of (140°–180°).

The experimental spectra of c.m. kinetic energies of protons and pions are compared in Fig. 6 to the distribution expected for the signal reaction $dd \rightarrow (^4$He-$\eta)_{\text{bound}} \rightarrow {}^3Hep\pi^-$. For further analysis we selected the kinetic energy of protons smaller than 200 MeV and of pions from the (180,400) MeV interval.

After the application of the described conditions the number of selected events in each excess energy (Q) interval was divided by the corresponding integrated luminosity and corrected for the reconstruction efficiency. The absolute value of the integrated luminosity in the experiment was determined using the $dd \rightarrow {}^3$Hen reaction and the relative normalization of points of the $dd \rightarrow {}^3$He$p\pi^-$ excitation function was based on the quasielastic proton-proton scattering [32].

The luminosity as a function of the excess energy is shown as triangles in Fig. 7 and is flat within the statistical
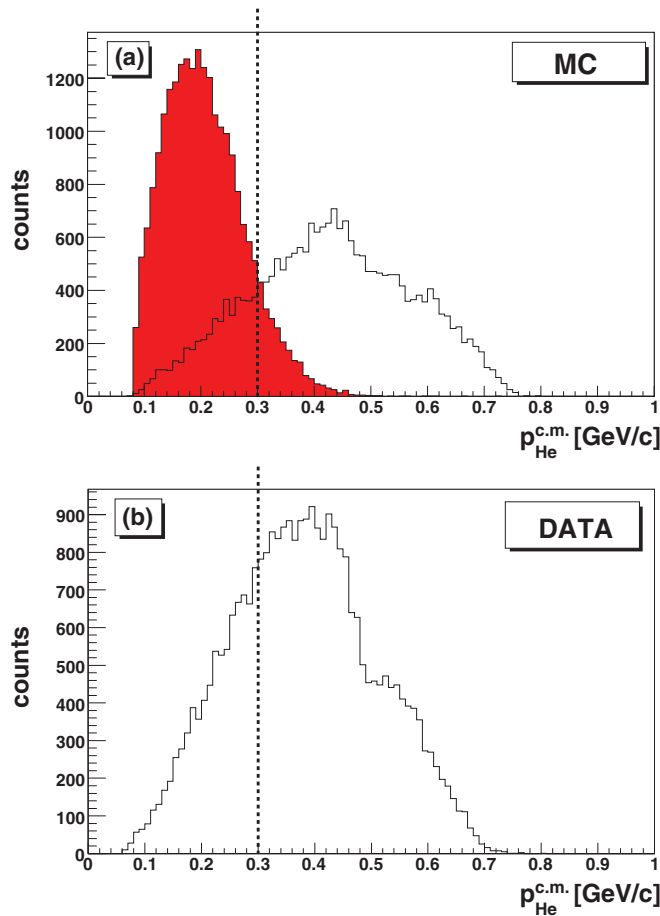
FIG. 3. (Color online) (a) Distribution of the ^{3}He momentum in the c.m. system simulated for the processes leading to the creation of the ^{4}He-η bound state: $dd \to (^4\text{He-}\eta)_{\text{bound}} \to {}^3\text{He}\,p\pi^-$ [red (gray) area] and of the phase-space $dd \to {}^3\text{He}\,p\pi^-$ reaction (black line). The simulation was done for a momentum of the deuteron beam of 2.307 GeV/c. The Fermi momentum parametrization was taken from Ref. [31]. (b) Experimental distribution of the ^{3}He momentum in the c.m. system. In both plots the dashed line demarcates the signal-poor and the signal-rich regions. The decrease of the counts at 0.48 GeV/c is due to the geometry of the border of the barrel and the endcaps of the scintillator barrel detector that was used in the p-π^- identification process. This region has no relevance in the next steps of the analysis.

FIG. 4. (Color online) Excitation function for the $dd \to {}^3\text{He}\,p\pi^-$ reaction for the signal-rich region corresponding to ^{3}He momentum below 0.3 GeV/c (a) and the signal-poor region with ^{3}He momentum above 0.3 GeV/c (b). The difference of the excitation functions for the signal-rich and signal-poor regions after the normalization to the second bin of Q is shown in panel c. The black solid line represents a straight-line fit. The threshold of ^{4}He-η is marked by the vertical dashed line.

uncertainties. The geometrical acceptance is about 60% and the overall efficiency including all selection conditions applied in the analysis is about 18% along the whole excess energy range. It is important to stress that both acceptance and efficiency are smooth and constant over the studied range.

The excitation function obtained after the selection criteria on energy and opening angles, the correction for the efficiency, and the normalization to the luminosity is presented in Fig. 8. It can be well described by a second-order polynomial (dashed line) resulting in a chi-squared value per degree of freedom of 0.98 and slightly worse by a straight line (solid line). As in the intermediat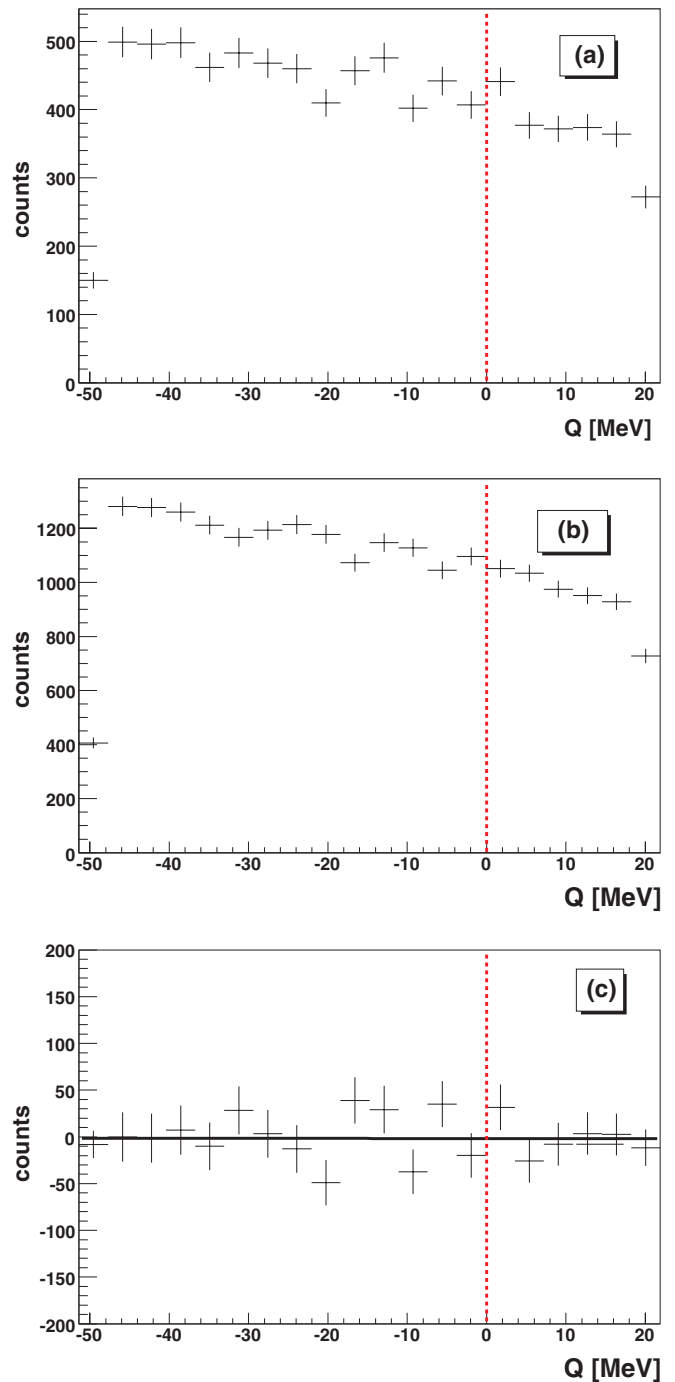e stage of the analysis (Fig. 4), the final excitation function exhibits no structure that could be interpreted as a resonance originating from the decay of the η-mesic ^{4}He.
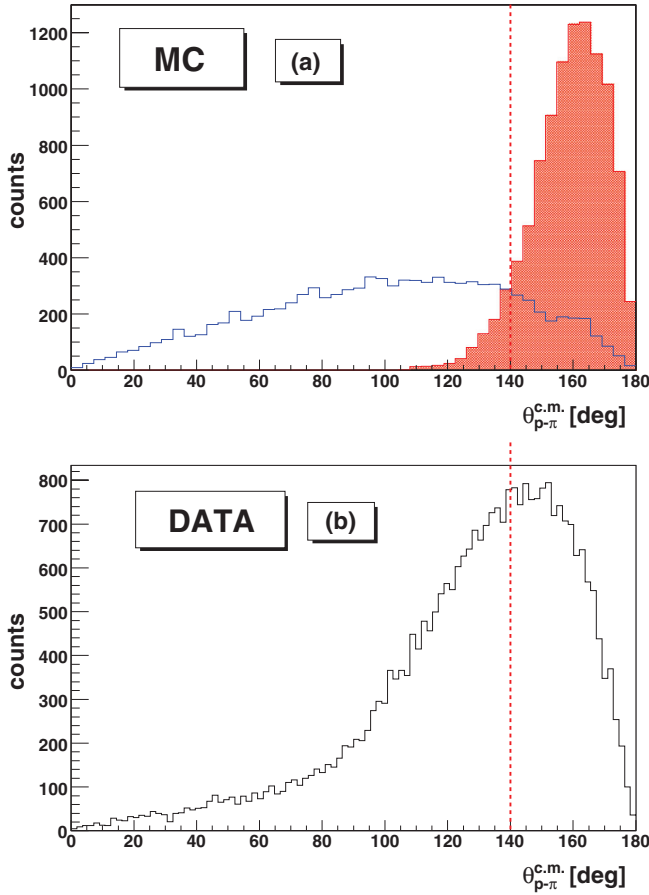
FIG. 5. (Color online) (a) Simulated distribution of the p-π^- opening angle in the c.m. system for the $dd \to (^4\text{He-}\eta)_{\text{bound}} \to$ $^3\text{He}\,p\pi^-$ reaction (red histogram) and for the phase-space $dd \to$ $^3\text{He}\,p\pi^-$ reaction [blue (solid) line]. (b) Experimental distribution of the p-π^- opening angle in the c.m. system. In both plots the red dashed line separates the signal-poor and the signal-rich regions.

FIG. 6. (Color online) Kinetic energy distribution of protons (a) and π^- (b) in the c.m. frame obtained from experiment (points) and from the simulations of a signal reaction (lines). The red dashed line indicates the boundary of the applied selection criteria: $E\text{kin}_p^{\text{c.m.}} <$ 200 MeV, $E\text{kin}_{\pi^-}^{\text{c.m.}} \in (180, 400)$ MeV. Please note that the ranges on the x axes are different.

III. UPPER LIMIT FOR THE $dd \to (^4\text{He-}\eta)_{\text{bound}} \to {}^3\text{He}\,p\pi^-$ CROSS SECTION

Since no signal originating from the formation of the ^{4}He-η bound state was observed, we estimate an upper limit for its production via the $dd \to (^4\text{He-}\eta)_{\text{bound}} \to {}^3\text{He}\,p\pi^-$ reaction. We assumed that a signal from the bound state in the excitation curve determined as a function of the excess energy Q with respect to the ^{4}He-η threshold can be described by a Breit-Wigner shape:

$$\sigma(Q, E_{\text{BE}}, \Gamma, A) = \frac{A\left(\frac{\Gamma}{2}\right)^2}{(Q - E_{\text{BE}})^2 + \left(\frac{\Gamma}{2}\right)^2}, \qquad (1)$$

where E_{BE} is the binding energy, Γ is the width of the bound state, and A is the cross section at the central energy ($Q = E_{\text{BE}}$) for the $dd \to (^4\text{He-}\eta)_{\text{bound}} \to {}^3\text{He}\,p\pi^-$ reaction. In this way, we assume that there is no interference between the signal and the nonresonant background. To determine an upper limit for the cross section for formation of the ^{4}He-η bound state and its decay into the $^3\text{He}\,p\pi^-$ channel we fitted the excitation function with a polynomial describing the background (first and second order) combined with the Breit-Wigner function.
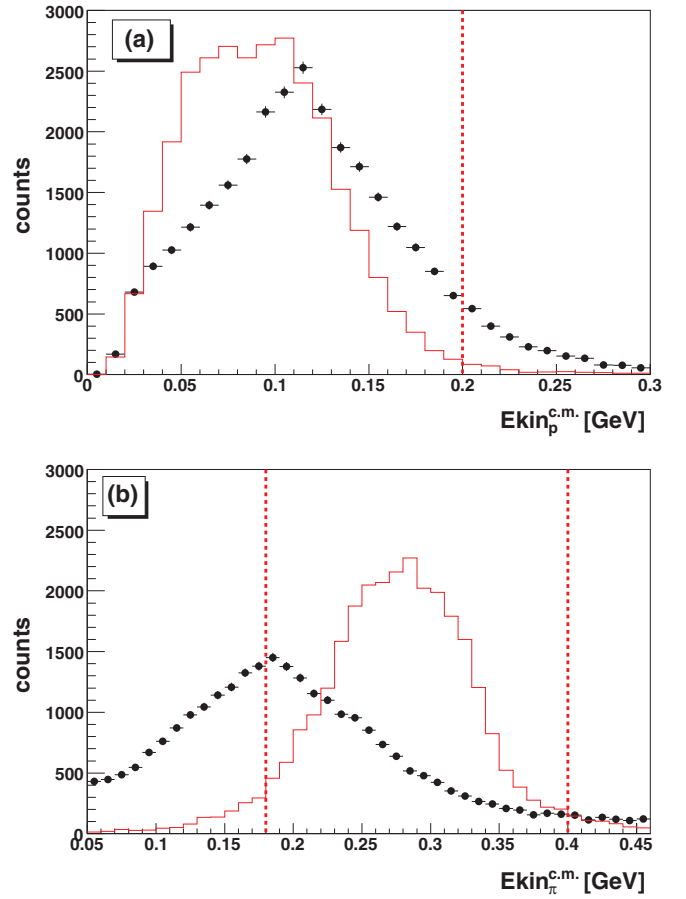
In the fit, the polynomial coefficients and the amplitude A of the Breit-Wigner distribution were treated as free parameters. The binding energy E_{BE} and the width Γ were fixed during the fit.

The fit was performed for various values of the binding energy and the width representing different hypothesis of the bound state properties. The binding energy and the width were varied in the range from 0 to -30 MeV and from 5 to 35 MeV, respectively. In each case, the extracted value of A is consistent with zero within the statistical uncertainties, which confirms the hypothesis of nonobservation of the signal.

To calculate an upper limit for the $dd \to (^4\text{He-}\eta)_{\text{bound}} \to {}^3\text{He}\,p\pi^-$ cross section, the standard deviation of the A values (σ_A) obtained from the above-described fit were multiplied by the statistical factor k equal to 1.281 55 corresponding to the probability confidence level (CL) of 90%. The final results were obtained by averaging the upper limits derived from fits with a background described by the second- and first-order polynomials.

The examples of the obtained upper limits are given in the last column of Table I. One can notice that these limits depend mainly on the width of the bound state but only slightly on the
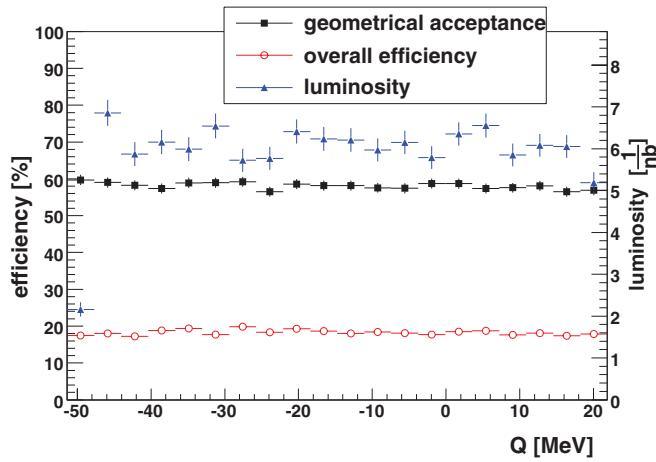
FIG. 7. (Color online) Geometrical acceptance (solid black squares), overall efficiency (open red circles), and luminosity (solid blue triangles) as a function of the excess energy. The right axis denotes the luminosity.

binding energy. The result for $E_{BE} = -20$ MeV is shown in Fig. 9.

IV. SYSTEMATICS

Systematic checks were performed by studying the sensitivity of the result to the variation of the selection conditions performed in the analysis and the assumption taken in the fitting procedure. Changing the range of the above-described selection conditions within $\pm 10\%$ gives a result consistent within the statistical uncertainties.

The smooth reconstruction efficiency and the luminosity dependency as a function of excess energy is of high importance because it eliminates the possibility of the creation of an artificial signal due to fluctuation of the acceptance or the luminosity. Two methods were applied to extract
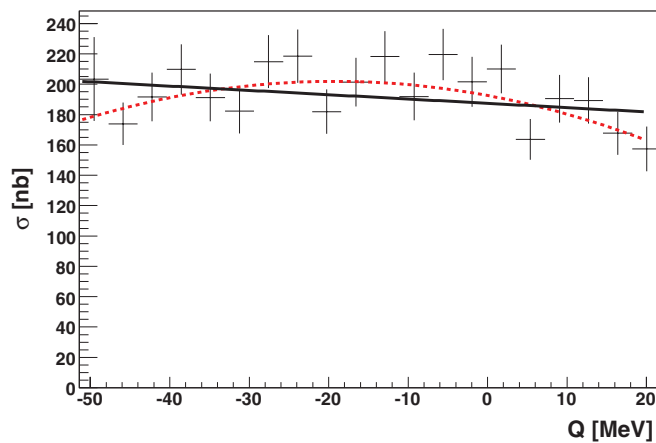

FIG. 8. (Color online) Experimental excitation function for the $dd \to {}^3\mathrm{He}\,p\pi^-$ reaction obtained after the normalization of the events selected in individual excess energy intervals by the corresponding integrated luminosities. The dotted and solid lines correspond to the second-order and the first-order polynomials fitted to the data.

TABLE I. The upper limit for the cross section for the bound state formation and decay in the process $dd \to ({}^4\mathrm{He}\text{-}\eta)_{\mathrm{bound}} \to {}^3\mathrm{He}\,p\pi^-$, determined on the 90% confidence level. The values were obtained from a fit of a Breit-Wigner function combined with first- and second-order polynomials (σ_{lin} and σ_{quad}, respectively) with different fixed values of binding energy E_{BE} and width Γ.

E_{BE} (MeV)	Γ (MeV)	σ_{quad} (nb)	σ_{lin} (nb)	$\frac{\sigma_{\mathrm{quad}}+\sigma_{\mathrm{lin}}}{2}$ (nb)
−30	10	21.57	20.87	21
−30	20	23.38	21.77	23
−30	30	28.83	25.33	27
−20	10	22.49	18.09	20
−20	20	25.94	16.96	21
−20	30	33.58	18.03	26
−10	10	23.86	18.51	21
−10	20	27.78	16.73	22
−10	30	36.88	17.48	27

the luminosity dependency as a function of Q. In addition to the normalization calculated on a bin by bin basis, we have estimated the luminosity dependence of Q using a fit of a first-order polynomial to the data. The results of both methods are in agreement. However, an overall normalization uncertainty of luminosity is equal to 11.5% [32] and this value is one of the contributions to the systematic uncertainty of the upper limit.

The description of the background shape with quadratic and linear functions produces additional systematic uncertainty, which is estimated as

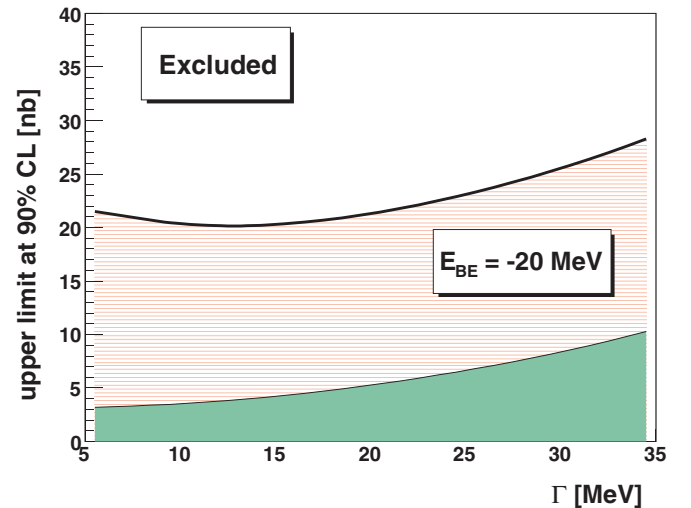$$\delta = \frac{(\sigma_{\mathrm{quad}} - \sigma_{\mathrm{lin}})}{2}. \tag{2}$$

FIG. 9. (Color online) Upper limit at 90% confidence level of the cross section for formation of the ${}^4\mathrm{He}\text{-}\eta$ bound state and its decay via the $dd \to ({}^4\mathrm{He}\text{-}\eta)_{\mathrm{bound}} \to {}^3\mathrm{He}\,p\pi^-$ reaction as a function of the width of the bound state. The binding energy was set to $E_{BE} = -20$ MeV. The green area at the bottom represents the systematic uncertainties.

The systematic error grows almost linearly with the assumed bound state width from about 5% ($\Gamma = 5$ MeV, $E_{BE} = -20$ MeV) to 33% ($\Gamma = 35$ MeV, $E_{BE} = -20$ MeV) and we take that range as an estimate of the systematic uncertainty due to the assumed shape of the background.

An important source of systematic errors comes from the Fermi momentum distribution of nucleons inside the ^{4}He nucleus applied in the simulations. We adapted the Fermi momentum parametrization described in Ref. [31], which is derived from the work of McCarthy *et al*. [33]. However, as it is shown in Ref. [34], the alternative derivation of the Fermi momentum distribution done by Nogga [35] is narrower by about 25%. Even if the choice of the given Fermi model does not influence the experimental method, it affects the overall acceptance of the ^{3}He ions in the forward detector and adds an additional systematic error of 8%.

In principle, a complete description would require the application of a momentum distribution with the embedded N^* resonance. However, up to now, such a description of the momentum distribution has been unavailable. Therefore, we approximate this distribution by Fermi momentum distribution of nucleons inside the ^{4}He nucleus. Adding the above-estimated contributions in quadrature we obtain systematic uncertainty of the upper limit that grows with the bound state width from 15% to 36%.

V. SUMMARY

We performed a search for the ^{4}He-η bound state via exclusive measurement of the excitation function for the $dd \rightarrow {}^3\mathrm{He} p \pi^-$ reaction. The measurement was carried out with the internal deuteron beam of the COSY accelerator scattered on a deuteron pellet target and with the WASA-at-COSY detection system used for registration of the reaction products. During the experimental run the momentum of the deuteron beam was varied continuously within each acceleration cycle from 2.185 to 2.400 GeV/c, crossing the kinematic threshold for η-meson production in the $dd \rightarrow {}^4\mathrm{He}\eta$ reaction at 2.336 GeV/c. This range of beam momenta corresponds to an interval of the excess energy in the ^{4}He-η system from -51.4 to 22 MeV.

For the first time in the experimental search for mesic nuclei all ejectiles were measured and the reaction was identified exclusively. No signal from η-mesic ^{4}He was observed. The upper limit for the cross section for the bound state formation and decay in the process $dd \rightarrow ({}^4\mathrm{He}\text{-}\eta)_{\mathrm{bound}} \rightarrow {}^3\mathrm{He} p \pi^-$ was determined on the 90% confidence level and it varies from 20 to 27 nb for the bound state width ranging from 5 to 35 MeV, respectively. The upper limits depend mainly on the width of the bound state and only slightly on the binding energy.

[1] A. M. Green and S. Wycech, Phys. Rev. C **71**, 014001 (2005).

[2] P. Moskal *et al*., Phys. Rev. C **69**, 025203 (2004).

[3] D. Jido, H. Nagahiro, and S. Hirenzaki, Phys. Rev. C **66**, 045202 (2002).

[4] T. Inoue and E. Oset, Nucl. Phys. A **710**, 354 (2002).

[5] S. D. Bass and A. W. Thomas, Acta Phys. Polon. B **41**, 2239 (2010).

[6] Q. Haider and L. C. Liu, Phys. Lett. B **172**, 257 (1986).

[7] B. J. Lieb *et al*., in *Proceedings of the International Nuclear Physics Conference, Sao Paulo, Brazil* (World Scientific, Singapore, 1989).

[8] G. A. Sokol *et al*., Fiz. B **8**, 85 (1999).

[9] A. Gillitzer, Acta Phys. Slov. **56**, 269 (2006).

[10] A. Budzanowski *et al*., Phys. Rev. C **79**, 012201(R) (2009).

[11] B. Krusche, F. Pheron, and Y. Magrbhi (Crystal Ball and TAPS Collaborations), Acta Phys. Polon. B **41**, 2249 (2010).

[12] W. Krzemien, P. Moskal, and J. Smyrski, Acta Phys. Polon. Supp. **2**, 141 (2009).

[13] M. Skurzok *et al*., Prog. Part. Nucl. Phys. **67**, 445 (2012).

[14] P. Moskal and J. Smyrski, Acta Phys. Pol. B **41**, 2281 (2010).

[15] J. Smyrski *et al*., Phys. Lett. B **649**, 258 (2007).

[16] T. Mersmann *et al*., Phys. Rev. Lett. **98**, 242301 (2007).

[17] W. Krzemien *et al*., Int. J. Mod. Phys. A **24**, 576 (2009).

[18] M. K. Anikina *et al*., arXiv:nucl-ex/0412036 (2004).

[19] H. Fujioka, Acta. Phys. Pol. B **41**, 2261 (2010).

[20] F. Pheron *et al*., Phys. Lett. B **709**, 21 (2012).

[21] K. Itahashi *et al*., Prog. Theor. Phys. **128**, 601 (2012).

[22] C. Wilkin *et al*., Phys. Lett. B **654**, 92 (2007).

[23] N. Willis *et al*., Phys. Lett. B **406**, 14 (1997).

[24] Q. Haider and L. C. Liu, Phys. Rev. C **66**, 045208 (2002).

[25] Q. Haider, Acta Phys. Pol. B Proc. Suppl. **2**, 121 (2009).

[26] C. Garcia-Recio *et al*., Phys. Lett. B **550**, 47 (2002).

[27] J. Smyrski, P. Moskal, M. Hodana, and W. Krzemien, Measurement of the $p + d$ and $d + d$ reactions near the η meson threshold for combined search of the η-He bound states and a precision measurement of the η meson mass, COSY Proposal 186, IKP, FZ Jülich, 2007.

[28] J. G. Fetkovich *et al*., Phys. Rev. D **6**, 3069 (1972).

[29] H.-H. Adam *et al*. (WASA-at-COSY Collaboration), arXiv:nucl-ex/0411038.

[30] D. Prasuhn *et al*., Installation and Commissioning of the Wasa Detector, IKP Annual Report, 2006.

[31] V. Hejny, Ph.D. thesis, Justus-Liebig University Gissen, 1998.

[32] W. Krzemien, Ph.D. thesis, Jagiellonian University, Krakow, 2011, arXiv:1202.5794 [nucl-ex].

[33] J. S. McCarthy *et al*., Phys. Rev. C **15**, 1396 (1977).

[34] M. Skurzok, M.Sc. thesis, Jagiellonian Univeristy, 2010, arXiv:1009.5503 [hep-ex].

[35] A. Nogga, Ph.D. thesis, Ruhr Universitat, Bochum, 2001.